SSC17-X-05

# Exploration of Energization and Radiation in Geospace (ERG): Development, Preliminary Flight Results, and Lessons Learned in JAXA's Small Science Satellite Project

Yosuke Nakamura, Takeshi Takashima, Seisuke Fukuda, Shin-ichiro Sakai, Iku Shinohara
Japan Aerospace Exploration Agency (JAXA)
Institute of Space and Astronautical Science (ISAS), JAXA, 3-1-1 Yoshinodai, Chuo-ku, Sagamihara, Kanagawa 252-5210 Japan; +81 90-7470-0304
nakamura.yosuke@jaxa.jp

## ABSTRACT

The Geospace explorer, the ERG satellite or nicknamed "ARASE" satellite, is the second satellite in the series of small science satellite program by Institute of Space and Astronautical Science (ISAS), Japan Aerospace Exploration Agency (JAXA). It was launched on December 20, 2016 by Epsilon launch vehicle. The satellite is now working quite well as designed, and preliminary mission data is being obtained. The purpose of the ERG project is to unravel how high energy electrons over MeV in the Earth's radiation belt (Van Allen Belt) are generated and lost by measuring interaction between plasma wave and electrically charged particles. To measure these physical processes in-situ, ERG dives into the center of the radiation belt. The orbit of ERG is highly elliptic; apogee altitude is approximately 32,000 km and perigee altitude is 440 km. In this paper, we introduce the scientific background and the outline of the satellite system design to effectively achieve the scientific observations with a small satellite standard bus. Then preliminary flight results are introduced, and finally lessons learned are discussed.

## INTORODUCTION

The region of outer space near the Earth, known as geospace, is populated by a large volume of very high-energy electrons and ions trapped in the Van Allen radiation belts by the Earth's magnetic field. These energetic highly charged particles cause a variety of problems such as the malfunctioning of the computers on satellites and undesirable charging of equipment, or radiation exposure to astronauts. In space storms, the outer belt electrons decrease significantly during the main phase, then recover to, and often increase over, prestorm levels during the recovery phase [1,2,3,4]. During huge magnetic storms, the radiation belts are largely deformed, and large flux enhancement are observed in the slot region and the inner belt [5].

Two possible mechanisms have been proposed for the acceleration of relativistic electrons. One is the external source process via quasi-adiabatic acceleration [6]. In this process, the energy of electrons increases due to the conservation of their first and second adiabatic invariants, when electrons are transported from the plasma sheet to the inner magnetosphere. This process has been modeled as the stochastic radial diffusion process, which is a fundamental transportation mode of energetic electrons. The ULF pulsations called "Pc5" with periods of a few minutes have been considered a main driver for the radial transportation via drift-resonance with electrons [7,8,9,10]. Another candidate is termed the internal acceleration process. It has been suggested that resonant interactions by whistler mode waves cause relativistic electron acceleration inside the radiation belts [11,12,13]. The free energy for generating whistler mode waves is the temperature anisotropy of electrons of tens of keV [14,15], and subsequent wave-particle interactions including nonlinear process will generate chorus waves [16,17] that accelerate relativistic electrons of the outer belt [18,19]. Figure 2 summarizes the transport/acceleration mechanisms in the L vs. energy diagram of the inner magnetosphere. L-value describes the set of magnetic field lines which cross the Earth's magnetic equator at a number of Earth-radii equal to the L-value.

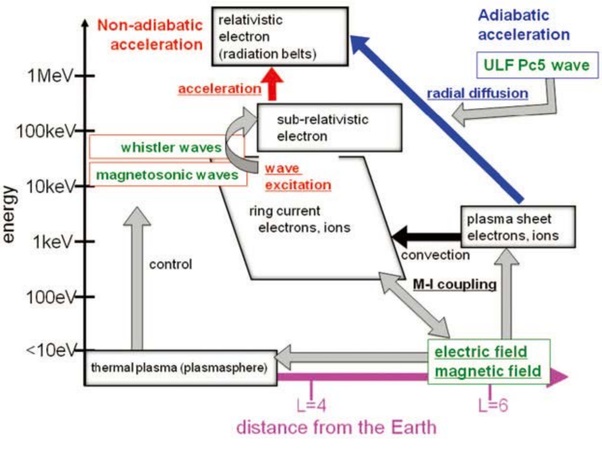


**Figure 1: Diagram of cross-energy coupling of the inner magnetosphere.**

## ERG PROJECT

### *Project Overview*

The purpose of the geospace exploration satellite, Exploration of energization and Radiation in Geospace (ERG), is to reveal how these high-energy electrons are accelerated and created, and how space storms develop [20]. Figure 2 depicts the ERG mission image of in-situ measurement of interaction between plasma wave and electrically charged particles. Since highly energized particles in the radiation belts can cause malfunctions of the computers on satellites and damage equipment through electrostatic charge, or threaten the astronauts with radiation exposure, space weather research for forecasting changes in geospace is an important aspect of this project.

Besides our Earth, other planets like Jupiter and Saturn also have radiation belts. A phenomenon known to be happening in various parts of the universe is that electrons are being accelerated close to the speed of light. The findings of the particle acceleration studies by the ERG satellite can also help unlock the mysteries of such particle acceleration occurring throughout the universe. In addition, the development of measuring instruments that can operate in powerful radiation environments will also be useful for the future exploration of planets with intense radiation belts, such as Jupiter.

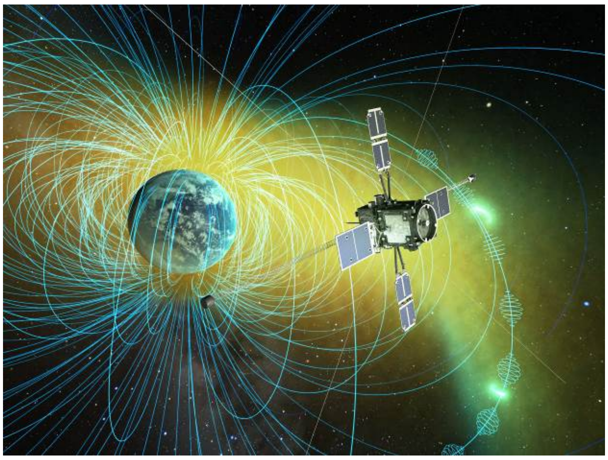

**Figure 2: In-situ measurement of interaction between plasma wave and electrically charged particles**

The concept of the ERG project was proposed in early 2000's by young scientists. Over many years' discussions, Institute of Space and Astronautical Science (ISAS), Japan Aerospace Exploration Agency (JAXA) selected ERG project for phase A study, conceptual design phase, as the second satellite in the series of small science satellite program in 2010. In 2012, after system definition review (SDR), the ERG was selected for a formal JAXA project to proceed phase B, the budget for the project was approved, and the ERG project team was organized. Preliminary Design Review (PDR) took place in 2013, Critical Design Review (CDR) in 2014. The ERG satellite was finally launched on December 20, 2016 by Epsilon launch vehicle from Uchinoura Space Center, and the satellite was nicknamed "ARASE".

### *Satellite, Ground Networks and Simulation Integrated Studies*

In order to understand the development of space storms and their effects that cause changes to the radiation belts, it is necessary to grasp what is occurring throughout the entire geospace region. In addition to detailed observation by the ERG satellite, the ERG project will combine remote sensing from ground networks with simulation and integrated analysis in order to comprehensively clarify the phenomena in this region.

Thus, the following teams are also involved in the ERG project: the satellite observation team, the ground-based network observations team, and the integrated data analysis/simulation team. The project science team and the project science center also work with project management.

### *ERG Satellite*

Figure 3 shows the appearance of the ERG satellite. The satellite consists of a bus module and a mission module. The bus module utilizes standardized small science satellite bus. The satellite deploys four solar array panels (SAP) just after its orbit insertion, and after the satellite was stabilized, four sets of 15m long wire antennas and two sets of 5m extensible masts are deployed. The attitude of the satellite is Sun-oriented and spin-stabilized around +Z axis with a spin rate of 7.5 rpm (spin period of 8 s).

The apogee altitude is approximately 32,000 km, located in the middle of the outer belt, and the perigee altitude is approximately 440 km. The orbital inclination is 32°, which is almost same as the latitude of the launch site. The satellite does not always observe at the magnetic equator. However, the satellite will have many chances for the observations near the equator and will measure the phase space density, generation of plasma waves, and accelerations of relativistic electrons, etc., near the equator.

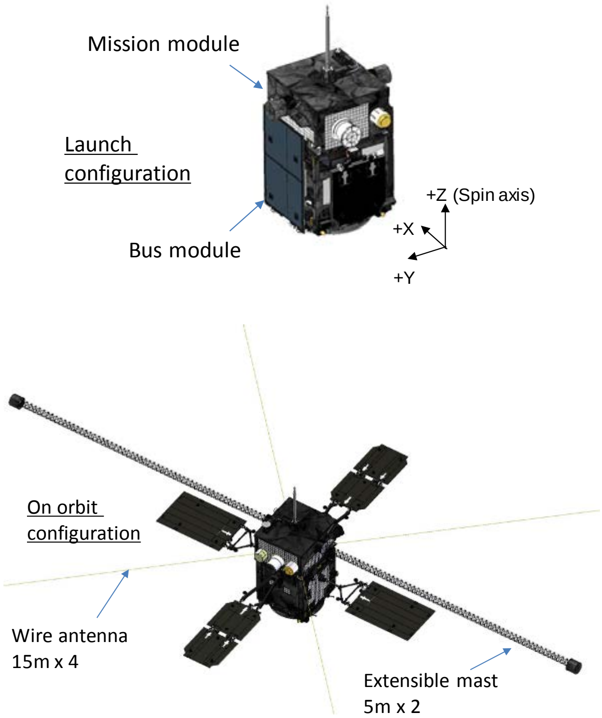


**Figure 3: Appearance of ERG satellite**

**Table 1: Mission instruments**

| Items | | Sensor | Energy range |
|---|---|---|---|
| Plasma and particle experiment (PPE) | Ion | Low-energy particle experiments - electron analyzer (LEP-e) | 10 eV - 19 keV |
| | | Medium-energy particle experiments - electron analyzer (MEP-e) | 10 keV - 80 keV |
| | | High-energy electron experiments (HEP) | 70 keV - 1 MeV, 700 keV - 2 MeV |
| | | Extremely high-energy electron experiments (XEP) | 400 keV - 20 MeV |
| | Electron | Low-energy particle experiments - ion mass analyzer (LEP-i) | 10 eV/q - 25 keV/q |
| | | Medium-energy particle experiments - ion mass analyzer (MEP-i) | 10 keV/q - 180 keV/q |
| Magnetic field and electromagnetic waves | | Magnetic Field Experiment (MGF) | - |
| | | Plasma Wave Experiment (PWE) | - |
| Wave particle interaction | | Software-type wave particle interaction analyzer (S-WPIA) | - |

### *ERG Mission Instruments*

Table 1 shows mission instruments installed in the ERG satellite. Comprehensive observations of plasma particles (electrons and ions), fields, and waves are important for understanding the cross-energy coupling for high-energy electron acceleration and dynamics of space storms. Instruments for plasma and particle experiment (PPE), magnetic field experiment (MGF), and plasma wave experiment (PWE) enables these observations. A cutting-edge technique for observing wave-particle interactions (software-type wave particle interaction analyzer, S-WPIA) can directly measure energy exchange processes between particles and plasma waves.

Plasma and particle experiment components such as MEP-e/i and LEP-e/i have 180 degree to 360 degree field of view within the mounting plane (+/- X plane) direction. Since the ERG satellite is spinning, those sensors have 4 $\pi$ steradian sphere shape field of views.

### *ERG Satellite System / Subsystems*

Figure 4 depicts system block diagram. Bold lines in the figure stand for SpaceWire network. There are three different SpaceWire networks within the ERG satellite system. The first one is for satellite management subsystem (SMS). A satellite management unit (SMU), a data recorder (DR), a telemetry and command interface module (TCIM), an attitude and orbit control processor (AOCP), a power control unit (PCU), a heater control unit (HCE), and a mission data processor electronics (MDP-E) are connected through a SpaceWire network router 1 (SWR1). The second network is for attitude and orbit control subsystem. Within the network, AOCP is connected to four attitude control interface modules (ACIMs), which are ACSSA, ACMDZ, ACANA, and ACVDI, through a SpaceWire network router 2 (SWR2). Each ACIM is connected to AOCS sensors and actuators respectively. The last one is for mission network. In the mission network, each mission instrument has a SpaceWire router, and consists ring-type network when considered in the aggregate system. Details of this mission network are described later in this paper.

Table 2 shows specifications of the satellite. The transponder of the satellite has four different transmission rates, 4k/64K/0.5M/1M bps, for telemetry downlink. Since the slant range between the satellite and ground stations varies greatly due to its highly elliptic orbit, these transmission rates are selected in an appropriate manner to maximize the amount of telemetry data. The reaction control subsystem (RCS) is used to increase the perigee altitude and to control attitude rate. For initial spin rate control and nutation

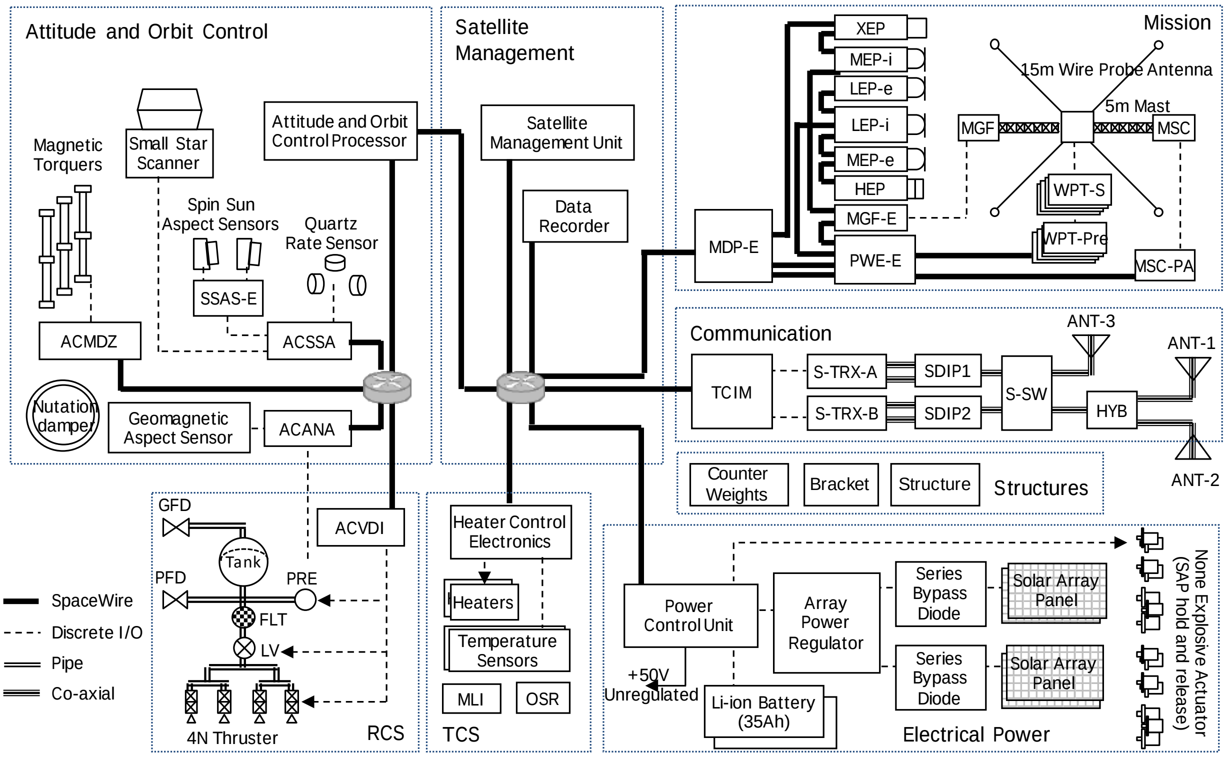


**Figure 4: System Block Diagram**

control, using quartz rate sensors (MEMS gyro) are used to feedback satellite attitude rate. Spin axis estimation is done on ground using data from spin-type sun aspect sensor (SSAS), geomagnetic aspect sensor (GAS), and small star scanner (SSC) [21].

**Table 2: System Specifications**

| Items | Specification |
|---|---|
| S/C Bus | Semi-standardized small science satellite bus |
| Mass | Approx. 355 kg (Wet)<br>Bus module:244 kg(Wet) 219 kg(Dry),<br>Mission module: 111 kg |
| Power | More than 700 W with four solar array panels<br>35 Ah Lithium ion battery |
| Size | Launch configuration: 1.5 m x 1.5 m x H2.7 m<br>After deployment: 31.2 m x 31.3 m x H2.7 m |
| Attitude | Spin stabilized |
| Communi-cation | S-band<br>4k/64K/0.5M/1M bps(downlink),<br>4k/256kbps(uplink) |
| Orbit | Highly elliptic orbit<br>Altitude of perigee: approx. 440 km<br>Altitude of apogee: approx. 32,000 km<br>Inclination 32 deg<br>Orbit period: about 570 minutes |
| RCS | 4N Hydrazine thruster x 4 |

### *Standardized Bus and its Modifications*

In the satellite bus module, we adopted spin-type standard bus for the small science satellite. By utilizing the same components applied in the first small science satellite SPRINT-A or “HISAKI”, which is the extreme ultraviolet space telescope for remote observation of the planets launched in 2012, the ERG project fully enjoy the benefits such as:

- The bus components fabrication period and system integration period was shortened compared with conventional ISAS science satellites.
- Recurrent production and short development period enables satellite development at lower cost.
- Recurrent production improves reliability of the satellite.

The SPRINT-A was the three-axis control inertially-fixed attitude LEO satellite, and the ERG is the spin-stabilized Sun pointing attitude satellite with highly elliptic orbit. The major differences in the system requirements of the ERG from APRINT-A are as follows:

1. The attitude is spin-stabilized. The attitude of the satellite is estimated on ground, and the spin axis

and spin rate control commands are planned on ground.

2. Mission orbit must be highly elliptic to cover inner and outer radiation belt.

3. After orbit insertion, the perigee altitude must be increased by delta-V maneuvers.

4. To measure electrically charged particles, magnetic field, and electro-magnetic waves, static charge on the satellite surface material must be prevented, and electro-magnetic compatibility (EMC) requirement is extremely severe to reduce noise on science data.

5. The satellite must tolerate severe environment such as high energy radiation in the outer radiation belt around apogee, and high flux atomic oxygen (AO) around perigee.

6. To reduce the weight of the satellite, single non-redundant bus components must be used except transponders. Instead, system level functional redundancies are preferred.

Although SPRINT-A and ERG both adopts same standard bus components, satellite system design was largely modified to meet these ERG specific requirements. ERG has two spin-type sun aspect sensors, a geomagnetic aspect sensor, and newly developed spin-type star scanner for offline attitude determination. Hydrazine thruster system is adopted to the ERG for delta-V and spin control, while SPRINT-A did not have thrusters. To meet EMC requirements, double shields are applied to the harnesses, EMC filters are added to the PCU. Black polyimide film is used as multi-layer insulation (MLI) surface material to prevent static charge. Other thermal control materials are also selected very carefully after many radiation and AO flux tests [22].

Even though there are differences on system design between SPRINT-A and ERG, standard small science satellite bus design is adopted to the network architecture using SpaceWire, data handling components and software, communication subsystem, electrical power subsystem, and structures. While customized flexibly based on different requirements, ERG satellite system has still its adequate quality utilizing advantage of the standard bus.

### *Mission System*

The mission module is mounted on the bus module as shown in Figure 3. Thermal and structural design is independent from bus system, and the interface are defined cleanly. Two sets of mission data processors / data recorders (MDP/MDR) installed in the MDP-E behave as gateways to the satellite management network. Figure 5 shows details of the mission SpaceWire ring-type network. In the network, each instrument has a CPU board which has a functionality of SpaceWire router and data processor. This architecture enables high speed data sharing within the mission components for integrated data analysis and system level redundancy.

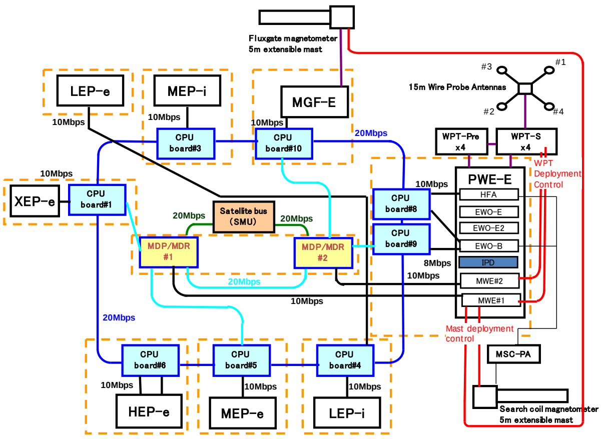


**Figure 5: Mission SpaceWire Network**

### *Development of ERG*

Figure 6 shows project schedule. After SDR, bread board models (BBM) and engineering models (EM) of mission components are designed and tested. A mechanical test model (MTM) and a thermal test model (TTM) of the mission module structure are also designed and tested to confirm the environmental conditions. The first system assembly, integration, and testing (AIT) was conducted in early 2015 using flight models and engineering models. The final AIT was conducted from October 2015 to September 2016.

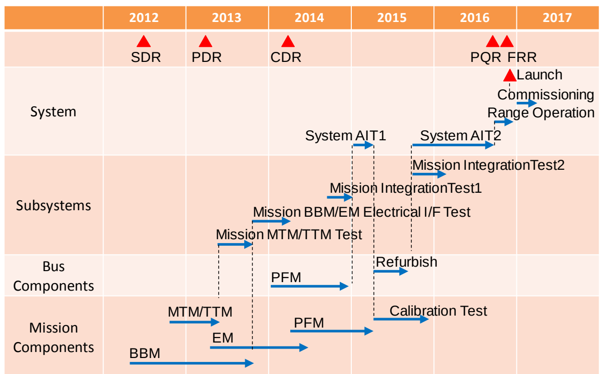


**Figure 6: Development Schedule**

## FLIGHT RESULTS

Figure 7 shows operation phase definition in ERG.

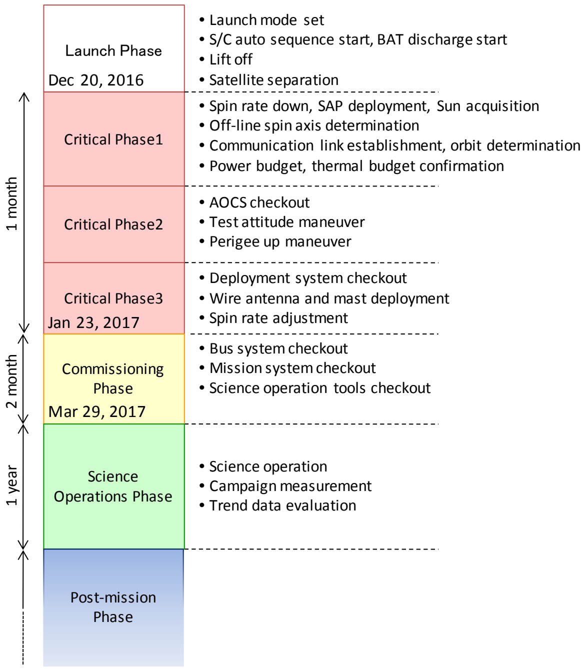


**Figure 7: Operation phase**

### *Launch Phase*

The second Epsilon Launch Vehicle with the ERG satellite aboard was launched successfully at 11:00 on December 20, 2016 from the Uchinoura Space Center. The launch vehicle flew as planned, and at approximately 13 minutes and 27 seconds after liftoff, the separation of ERG was confirmed. The signals were received in the Santiago Ground Station, the Republic of Chile at 11:37.

**Figure 8: Epsilon L/V lift-off**

### *Critical Operation Phase*

The critical operation phase is divided into three detailed phase. In the first phase, the ERG completed spin-down and active nutation control, SAP deployment, and Sun acquisition. Figure 9 shows the ground track of the ERG. The first apogee pass was over the Southern Hemisphere, and the pass duration at the Santiago Ground Station was nearly 9 hours. The second apogee pass was operated at the ground stations in Japan. But the pass duration was still nearly 9 hours so that we could have enough time to check the satellite status. During this period operation team confirmed communication link establishment, power and thermal budget, and determined its orbit. It took almost three days.

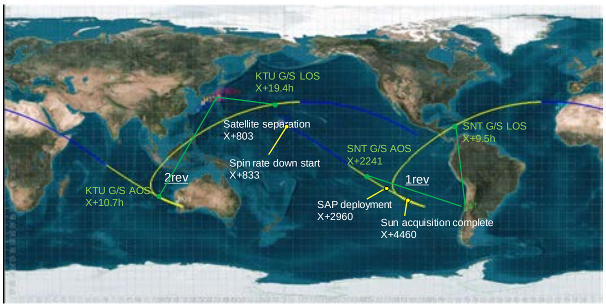


**Figure 9: Ground track during critical operation phase 1**

In the second phase, we conducted perigee up delta-V maneuvers. Before the maneuvers, we conducted AOCS functions checkout step by step, which include test attitude maneuvers and a test delta-V maneuver. Actual delta-V maneuvers were conducted twice to reduce maneuver control error risks, and perigee altitude was increased from 214km to 460 km.

15m wire antennas deployment and 5m extensible masts deployment were conducted in the third phase. Because these wire antennas and masts are flexible structures, deployment operations were also conducted step by step paying maximum attention to the attitude of the satellite. Finally, spin rate of the satellite was adjusted to 7.5 rpm using thrusters. The entire critical operation phase took one month.

### *Commissioning Phase*

In commissioning phase, we conducted subsystem functions and performance checkout, initial start-up of mission instruments including high voltage power supply. In order to avoid electrical discharge in the insufficient vacuum condition by outgassing, we had to wait at least one month before turning high voltage ON. After all mission components were started-up and initial mission data was confirmed, we conducted operation training, checked operation planning and verification tools, and modified satellite parameters to prepare for science operation phase.

### *Science Operation Phase*

In March 24, 2017, ERG project finished the commissioning phase and started the science operation phase. Figure 10 shows operation image of the ERG in highly elliptic orbit. The ERG is mainly operated using ground stations at Uchinoura (34 m and 20 m diameter), Katsuura (20 m diameter), and Okinawa (18 m diameter) because large antenna dishes are required for high speed communication around apogee. Science data is recorded continuously to the mission data recorder. In addition, huge burst mission data is recorded when space storms or other space events happen. Thus, most of the long pass window around apogee above Japan is used to downlink mission data with high speed (1 Mbps or 0.5 Mbps) S-band. On the other hands, satellite ranging for orbit determination is also important since altitude of perigee is so low that orbit perturbations are not negligible due to the air drag. Ranging operations are mainly conducted around perigee with low speed (4 kbps or 64 kbps) S-band.

In order to synchronize science data among multiple instruments, so called Index Pulse (IP) is distributed from AOCP. An IP is normally generated from a Sun detection pulse generated by SSAS per every one spin. But when the satellite is in the shadow of the Earth, IP generation mode must be changed to the auto IP mode.

Sun direction moves approximately 1 degree per day due to the Earth revolution about the Sun. Thus, spin axis must be controlled to track the Sun. During the science operation phase, RCS is not used for this spin axis control operation. Instead, magnetic torquers (MTQ) are used in order not to excite the vibration or liberation by flexible structures such as wire antennas and extensible masts. Furthermore, because the orbit is highly elliptic, MTQ control is effective only when the altitude of the satellite is lower than 3,000 km where Earth's magnetic field is enough strong. On the other hands, driving MTQs makes magnetic noise to the science instruments so that drive duration must be minimized and demagnetization operation is required when MTQ is used.

The ERG satellite is now in good condition, and obtaining excellent science data. A campaign observation from the end of March to the beginning of May 2017 was conducted and the data is being provided to scientists for detailed analyses.

## LESSONS LEARNED

### *Utilizing Standardized Bus*

The ERG satellite was second satellite in the series of small science satellite program so that we could enjoy a considerable amount of benefits shown below from standardized bus concept.

- Troubles during components and satellite system development could be greatly reduced.
- Satellite telemetry and command design and definitions database could be reused.

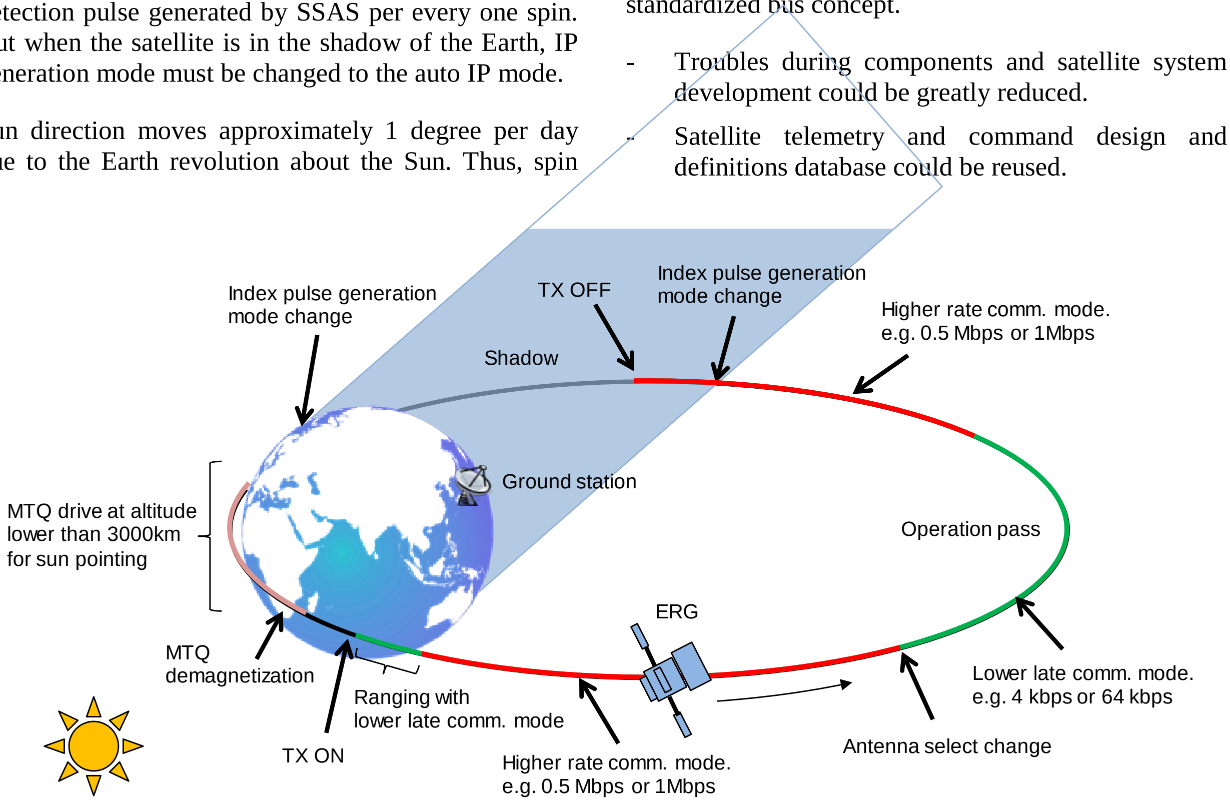


**Figure 10: Operation image of the ERG in highly elliptic orbit**

- The MTM of the bus module was already tested in the first satellite project. Thus, we had only to test mission module MTM, and the test could be very quick and compact.
- People in charge of bus subsystems, such as the communication subsystem and electrical power subsystem, could be less involved in the ERG project by adopting same bus components.
- Ground test and operation system was also standardized. We call it "Generic Spacecraft Test and Operations Software (GSTOS)". This software greatly reduced efforts to develop ERG's test and ground system. The ERG specific function could be defined within the GSTOS.

On the other hands, sticking too much to standardized generic system may restrict flexibility to meet the mission specific requirements. In the standard science bus design, material of heat radiation plane was silver Teflon. But considering severe radiation and AO flux environmental conditions, optical solar reflectors (OSR), which is more expensive than silver Teflon, were preferred for the material. We finally selected OSRs for the thermal control material, but we had to conduct thermal analysis again to change thermal design. Determining reasonable balance between standardized bus design and mission modification is the key to the efficient development and mission success.

***Leveraging the Value of the Small Satellite***

Small science satellite program was started to maximize the scientific value with reasonable cost, schedule, and quality. Project team is not so big that everyone in the team conducts design, analysis, and testing. But once the project started, people within our organization become increasingly aware of qualities, documentations and administrative procedures. This makes the project cost larger and schedule longer, and the project may lose its merits.

Collocating the team is also important rule of the small satellite project. In ISAS / JAXA, researchers in the project have their own rooms. So, we had to communicate each other mainly using emails, and sometimes this caused miscommunications and gaps of information among the team members. After system integration phase, the ERG project people get together in a test building, and this problem was resolved.

***Maximizing Downloaded Data in Elliptical Orbit***

Because the orbit is highly elliptical, the distance between the satellite and ground stations changes greatly, and it follows that free space loss of RF signal changes greatly. In certain attitude and look angle to the ground stations, antennas must be switched to avoid null antenna gain. With these situations, the downlink rate, RF power, and antennas had to be configured appropriately in a timely manner to maximize the overall downloaded mission data. These kinds of operation planning are complicated multidiscipline engineering.

To solve the problem, we developed two types of command planning software which calculate timings of changing communication modes. The first one uses fast and robust simple algorithm, but the amount of downloaded mission data is not maximized. The second one uses optimal algorithm called Graph-Theoretic Approach [23]. In orbit, we conducted the satellite's antenna pattern estimation, and calculated communication link margins to modify the software. Finally, both algorithm worked well, and we could obtain a large amount of mission data.

***Operation Training using the AOCS Simulator***

Although the ERG is spin-stabilized attitude satellite, there were several difficulties in the attitude control operations such as:

- Spin balance, i.e. moment of inertia ratio (MOIR) of the satellite was unstable in launch configuration, and that might cause flat spin if some failures occurred.
- Direction of the spin axis had to change largely in delta-V maneuvers. Changing the spin axis might induce a large nutation motion.
- Deploying flexible structure might induce librational coupling motion between the natural frequencies of the structure and spin or nutation frequencies.

To prepare for these failure modes, the AOCS team conducted operation trainings using the static closed loop test (SCLT) setups shown in Figure 11. The trainings were very effective. In the real operations, there was no failure in the AOCS as a result. But AOCS team could fully prepare for emergency operations

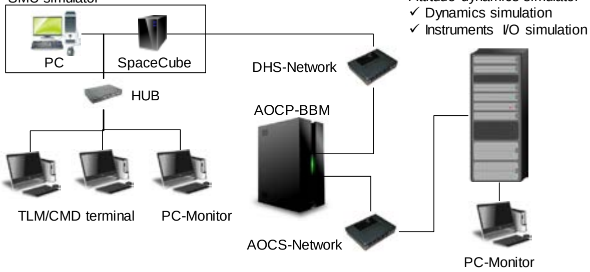


**Figure 11: AOCS operation training using static closed loop test equipment and operation system**

## REFERENCES


1. Baker, D. N., J. B. Blake, R. W. Klebesadel, and P. R. Higbie (1986), Highly relativistic electrons in the Earth's outer magnetosphere, 1. Lifetimes and temporal history 1979–1984, J. Geophys. Res., 91(A4), 4265–4276 .
2. Nagai, T. (1988), "Space weather forecast": Prediction of relativistic electron intensity at synchronous orbit, Geophys. Res. Lett., 15(5), 425–428.
3. Reeves, G. D., et al (1998), The relativistic electron response at geosynchronous orbit during the January 1997 magnetic storm, J. Geophys. Res., 103(A8), 17,559–17,570.
4. Miyoshi, Y., and R. Kataoka (2005), Ring current ions and radiation belt electrons during geomagnetic storms driven by coronal mass ejections and corotating interaction regions, Geophys. Res. Lett., 32, L21105.
5. Baker, D. N., et al (2004), An extreme distortion of the Van Allen belt arising from the 'Halloween' solar storm in 2003, Nature, 432, 878–881.
6. Schulz, M., and L. Lanzerotti (1974), Particle Diffusion in the Radiation Belts, Springer, Berlin.
7. Rostoker, G., S. Skone, and D. N. Baker (1998), On the origin of relativistic electrons in the magnetosphere associated with some geomagnetic storms, Geophys. Res. Lett., 25(19), 3701–3704.
8. Hudson, M. K., et al (2001), Radiation belt electron acceleration by ULF wave drift resonance: Simulation of 1997 and 1998 storms, in Space Weather, Geophys. Monogr. Ser., vol. 125, edited by P. Song, H. J. Singer and G. L. Siscoe, pp. 289–296, AGU, Washington, D. C.
9. Elkington, S. R. (2006), A review of ULF interactions with radiation belt electrons, in Magnetospheric ULF Waves: Synthesis and New Directions, Geophys. Monogr. Ser., vol. 169, edited by K. Takahashi et al., pp. 177–193, AGU, Washington, D. C.
10. Mathie, R. A., and I. R. Mann (2000), A correlation between extended intervals of Ulf wave power and storm-time geosynchronous relativistic electron flux enhancements, Geophys. Res. Lett., 27(20), 3261–3264.
11. Summers, D., R. M. Thorne, and F. Xiao (1998), Relativistic theory of wave-particle resonant diffusion with application to electron acceleration in the magnetosphere, J. Geophys. Res., 103(A9), 20,487–20,500.
12. Miyoshi, et al (2003), Rebuilding process of the outer radiation belt during the 3 November 1993 magnetic storm: NOAA and Exos-D observations, J. Geophys. Res., 108(A1), 1004.
13. Horne, R. B., et al (2005), Timescale for radiation belt electron acceleration by whistler mode chorus waves, J. Geophys. Res., 110, A03225.
14. Kennel, C. F., and H. E. Petschek (1966), Limit on stably trapped particle fluxes, J. Geophys. Res., 71(1), 1–28.
15. Jordanova, V. K., R. M. Thorne, W. Li, and Y. Miyoshi (2010), Excitation of whistler mode chorus from global ring current simulations, J. Geophys. Res., 115, A00F10.
16. Katoh, Y., and Y. Omura (2007), Computer simulation of chorus wave generation in the Earth's inner magnetosphere, Geophys. Res. Lett., 34, L03102.
17. Omura, Y., Y. Katoh, and D. Summers (2008), Theory and simulation of the generation of whistler-mode chorus, J. Geophys. Res., 113, A04223
18. Summers, D., and C. Ma (2000), A model for generating relativistic electrons in the Earth's inner magnetosphere based on gyroresonant wave-particle interactions, J. Geophys. Res., 105(A2), 2625–2639.
19. Summers, D., B. Ni, and N. P. Meredith (2007), Timescales for radiation belt electron acceleration and loss due to resonant waveparticle interactions: 1. Theory, J. Geophys. Res., 112, A04206.
20. Miyoshi, Y., et al (2012), The Energization and Radiation in Geospace (ERG) Project, Dynamics of the Earth's Radiation Belts and Inner Magnetosphere Geophysical Monograph Series 199.
21. Soken, H. E., et al (2017), Spin Parameters and Nonlinear Kalman Filtering for Spinning Spacecraft Attitude Estimation, 2017 Space Flight Mechanics Meeting, San Antonio, AAS 17-249.
22. Shibano, Y., et al (2015), Thermal performance degradation of spacecraft radiator by outgassing of adhesives in space environment, the 13th International Symposium on Materials in the Space Environment, Pau.

23. Someya, K., et al (2017), A Graph-Theoretic Approach to Optimal Planning of Satellite Downlink, 31st International Symposium on Space Technology and Science (ISTS), Matsuyama, 2017-n-03.